Efficient degradation of tetracycline by ultraviolet-based activation of peroxymonosulfate and persulfate

Jiamin Hu, Jing Zhang, Qingguo Wang, Qian Ye, Hao Xu, Guanyu Zhou and Jinfeng Lu

ABSTRACT

In this study, the difference in oxidative capacity for removing antibiotics and the mechanism between the Cu(II)/peroxymonosulfate (PMS)/UV and Cu(II)/persulfate (PDS)/UV systems were compared under various conditions. The optimal Cu(II) concentration in the Cu(II)/PMS/UV system was 30 μM, and in the Cu(II)/PDS/UV system was 50 μM. With the PMS or PDS concentration increasing, higher tetracycline (TC) degradation in these two systems occurred. Investigation on the mechanism revealed that •OH was the primary radical in the Cu(II)/PMS/UV system, while $SO_4^{\bar{}}$• was the primary radical in the Cu(II)/PDS/UV system where •OH also played an important role. In these two systems, it was observed that Cu(I) was generated by PMS or PDS activated via UV illumination; however, oxygen alone could not promote TC removal. The degradation of TC was increased with the increasing pH level. In addition, TC degradation in the Cu(II)/PMS/UV system followed the pseudo-first-order kinetics model during the entire reaction period. It was found that the TC degradation kinetics in the Cu(II)/PDS/UV system can be divided into two parts (0 to 7 min and 10 to 50 min) and these two parts had good agreement with the pseudo-first-order kinetics model, respectively.

Key words | copper, hydroxyl radicals, sulfate radical, tetracycline, UV

Jiamin Hu
Jing Zhang (corresponding author)
Qingguo Wang
Qian Ye
Hao Xu
Guanyu Zhou
College of Architecture & Environment,
Sichuan University,
Chengdu 610065,
China
E-mail: *zjing428@163.com*

Jinfeng Lu
College of Environmental Science and Engineering,
Nankai University,
Tianjin 300071,
China

INTRODUCTION

There is increasing attention to the presence of pharmaceuticals in the aquatic environment, due to the great negative impact on human health and the ecosystem (Kuster & Adler 2014; Natija *et al.* 2017). Among various pharmaceutics, tetracycline (TC), a common type of antibiotics, is widely used to treat human and animal diseases and in the animal husbandry and fisheries fields (Shi *et al.* 2017; Zhou *et al.* 2017). However, TC is difficult to be metabolized completely by humans and animals and finds its way into the water system (Natija *et al.* 2017; Shi *et al.* 2017). Traditional methods such as electrochemistry and adsorption can remove TC (Oturan *et al.* 2013; Zhang *et al.* 2011; Wu *et al.* 2016). Additionally, ultraviolet (UV)-based advanced oxidation processes (AOPs) have been shown to effectively degrade pharmaceuticals. TC photolytic degradation has also been reported in recent years, attracting more and more attention because of the high efficiency in removing refractory compounds (Zhang & Li 2014; Ai *et al.* 2015; Sun *et al.* 2016; Xiao *et al.* 2017).

Sulfate radical ($SO_4^{\bar{}}$•), generated from the activation of peroxymonosulfate (PMS) by UV, transition metals and heat (Anipsitakis & Dionysiou 2004; Cui *et al.* 2016; Jorge *et al.* 2017; Yang *et al.* 2017), have been shown to be effective in treating pharmaceuticals due to the high redox potential (2.5–3.1 V), compared with hydroxyl radical (•OH, 1.9–2.7 V) (Buxton *et al.* 1988; Yang *et al.* 2014; Zhang *et al.* 2015; Ye *et al.* 2017). Many studies found that the combination of ultraviolet and transition metals like Fe(II) and Co(II) can strongly enhance the oxidation capacity of a single system (Khan *et al.* 2016; Jorge *et al.* 2017). For instance, Fe(II) activates PMS to produce Fe(III) at first, and then Fe(II) regenerated via the reaction between Fe(III) and UV, indicating that UV promotes the transformation of the iron-redox cycle. Meanwhile, $SO_4^{\bar{}}$• is produced and aims to remove the organic compounds. The reaction

doi: 10.2166/wst.2019.034

is grown in Equations (1) and (2) as follows (Khan *et al.* 2016):

$$Fe^{2+} + HSO_5^- \rightarrow Fe^{3+} + SO_4^- \cdot + OH^- \ (k = 3.0 \times 10^4\ M^{-1}\ s^{-1}) \quad (1)$$

$$Fe(OH)^{2+} + h\nu \rightarrow \cdot OH + Fe^{2+} \quad (2)$$

Although iron is the most common transition metal in wastewater treatment, there are some drawbacks in iron-based AOPs. The most obvious one is the limitation of the pH level due to the precipitation of Fe^{2+}/Fe^{3+} (Khan *et al.* 2016). Other metals like copper have drawn wide concern recently in overcoming this shortcoming, because the solubility product (k_{sp}) of $Cu(OH)_2$ (1.6×10^{-19}) is much higher than $Fe(OH)_3$ (2.5×10^{-35}) (Meighan *et al.* 2008; Kang *et al.* 2014). It shows that copper is not easy to precipitate at neutral or alkaline conditions compared with iron. Moreover, Verma *et al.* (2016) reported that the addition of Fe^{3+} in a PMS/UV system was found to be more efficient in the degradation of anatoxin-a. Furthermore, cuprous copper (Cu(I)) is considered as a promising catalyst and has a high potential to activate the other oxidation agents like oxygen (O_2), hydrogen peroxide (H_2O_2) and PMS, but it is easily oxidized to cupric copper (Cu(II)) (Yuan *et al.* 2012, 2013). Thus, copper is seldom used in wastewater treatment.

Similar to PMS, peroxydisulfate (PDS) can also be activated by UV to generate $SO_4^-\cdot$. Zhang's study showed that the AOP's performance in removing pharmaceuticals was higher with PDS/UV than H_2O_2/UV (Zhang *et al.* 2015). In addition, the sulfate radical was produced through combining Fe(II) with PDS according to Equation (3).

$$S_2O_8^{2-} + Fe^{2+} \rightarrow SO_4^- \cdot + Fe^{3+} + SO_4^{2-} \ (k = 2 \times 10\ \ M^{-1}\ s^{-1}) \quad (3)$$

Most previous studies used reducing agents like hydroxyl amine (HA) to reduce the transition metals (Lee *et al.* 2016). Based on Equation (2), it has been verified that UV is also capable of reducing high valence transition metal ions to low valence transition metal ions (Bedoui *et al.* 2011; Liu *et al.* 2016a, 2016b). As oxidation agents and transition metals simultaneously exist, on the one hand, the addition of UV directly activates oxidation agents like PMS and PDS to produce free radicals (Lou *et al.* 2016; Liu *et al.* 2016a, 2016b). On the other hand, UV continuously reduces transition metals that are oxidized by oxidation agents, forming a metal cycle with high and low valence ions (Wu *et al.* 1999; Bedoui *et al.* 2011). Thus, it is reasonable to consider that Cu(II) may be reduced to Cu(I) via UV first, and then Cu(I) activates PMS or PDS to promote the production of radicals like $SO_4^-\cdot$ and $\cdot OH$, which further enhance the oxidative ability of the Cu(II)/PMS or Cu(II)/PDS systems.

This study compares and evaluates the efficiency of removing the pharmaceuticals TC in Cu(II)/PMS/UV and Cu(II)/PDS/UV systems. The objects of this study are: (1) to compare the oxidative capacity for removing TC in different systems; (2) to examine the effect of Cu(II) concentration, PMS and PDS concentration in the two systems; (3) to determine the mechanism of radicals generation and investigate the species of radicals in different systems.

MATERIALS AND METHODS

Materials

Potassium peroxymonosulfate (PMS) and copper sulfate pentahydrate ($CuSO_4 \cdot 5H_2O$, ≥99.0%) were supplied by Sigma-Aldrich. Tetracycline (TC) was bought from Aladdin. Sodium persulfate (PDS, ≥99.0%), neocuproine hemihydrate (NCP, ≥98%), sulfuric acid (H_2SO_4, 75%), sodium hydroxide (NaOH, ≥96%) and coumarin (≥98%) were supplied by Sinopharm Chemical Reagent Co., Ltd. Tert-butyl alcohol (TBA, ≥99.5%) and ethyl alcohol (EA, 75%) were bought from Kelong chemical reagent factory. All of the reagents above were of analytic purity. Pure oxygen (O_2, ≥99.2%) and pure nitrogen (N_2, ≥99.9%) were stored in special high-pressure gas cylinders. Methanol and ammonium acetate were chromatographically pure and were bought from Sinopharm Chemical Reagent Co., Ltd (China).

Experimental procedure

All experiments were performed in a 500 mL tailor-made columniform glass container with a quartz tube of 35 mm diameter. A 25 W low pressure (LP) ultraviolet lamp peaking at 254 nm was placed in the quartz tube. During the experiments, samples in the container were surrounded and cooled by condensate water in order to keep the temperature of the samples constant at the room temperature. Cu(II) ($CuSO_4 \cdot 5H_2O$) and TC at the desired concentrations were spiked into 500 mL pure water. The initial pH was adjusted by 0.5 M H_2SO_4 or 1.0 M NaOH. Oxygen or nitrogen was bubbled into the samples at 1.0 L·min^{-1} for 20 min

before the experiments, and was then set at 0.5 L•min^{-1} during the experiments. Each run was started by PMS or PDS addition and UV light emition. TBA and EA, the scavengers of •OH and SO_4^{-}•, were added to the samples immediately after UV emition in the quenching experiments, respectively. Samples with coumarin were quenched by $NaNO_2$ after being withdrawn and then were detected by high performance liquid chromatography (HPLC).

Analysis methods

The concentration of TC was detected at 357 nm by a UV-vis spectrometer (MAPADA, UV-1800) (Shi *et al.* 2017). The concentration of Cu(I) was spectrophotometrically measured by the neocuproine method (American Public Health Association 2005). In addition, the concentration of dissolved oxygen (DO) was determined by a dissolved oxygen meter (JPB-607A). A pH meter (pHs-25) was used to detect the pH level and the dates changed less than ±0.1. Each experiment was replaced three times at the same conditions and the standard deviation was less than 2%.

The product of coumarin and •OH, 7-hydroxycoumarin (7OHC), was determined by HPLC (Waters e2695, USA) equipped with a reverse-phase C18 column (4.6 × 150 mm). The mobile phases were methanol and 0.1% ammonium acetate (50:50, v/v). The analysis conditions were as follows: the excitation wavelength: 346 nm; the determination wavelength: 456 nm; the column temperature: 30 °C; the injection speed: 1 mL/min (Louit *et al.* 2005; Takuya *et al.* 2011; Zhou *et al.* 2019).

RESULTS AND DISCUSSION

Oxidative degradation of TC

To investigate the efficiency of different systems, experiments for removing TC were examined at pH 3.5 in the PMS, PDS, UV, Cu(II), Cu(II)/UV, PMS/UV, PDS/UV, Cu(II)/PMS/UV and Cu(II)/PDS/UV systems, respectively. As shown in Figure 1, TC removal was 49.3%, 71.8% and 93.1% in the PMS, PMS/UV and Cu(II)/PMS/UV systems (top). Through these results, it was found that the addition of UV (PMS/UV) increased TC degradation of the PMS system more than 20%. Besides, TC degradation of the Cu(II)/PMS/UV system was increased by over 20% than that in the PMS/UV system, indicating that the addition of Cu(II) and UV could strongly enhance the oxidative capacity of the PMS system. The degradation of TC in the PDS, PDS/UV and Cu(II)/PDS/UV systems (bottom) were 17.1%, 40.7% and 67.1%, which was similar with the former results of PMS. Moreover, single Cu(II), single UV and Cu(II)/UV systems could not remove TC during the 50 min reaction period.

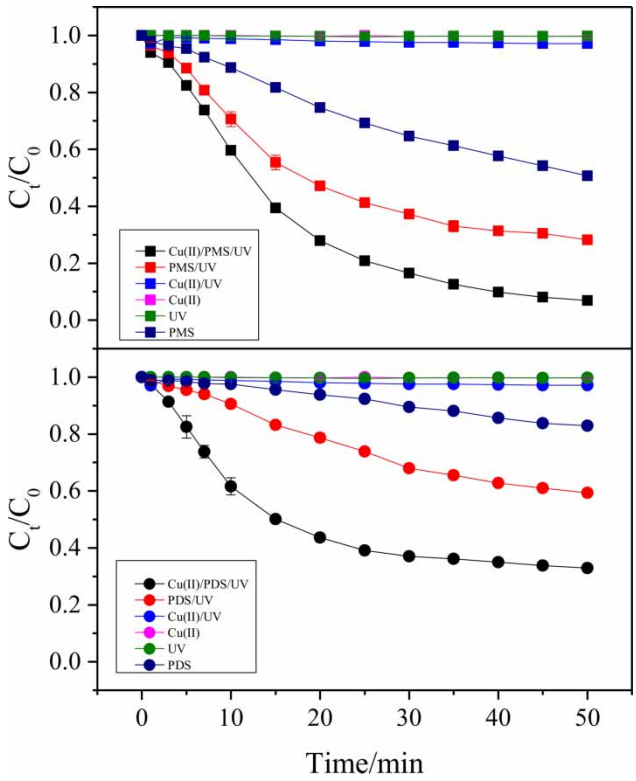

Figure 1 | Oxidative degradation of TC by PMS (top) and PDS (bottom) activated. Experimental conditions: $[Cu(II)]_0 = 20$ μM; $[PMS]_0 = [PDS]_0 = 0.50$ mM; $[TC]_0 =$ 9 mg/L; pH = 3.5; $T_0 = 25$ °C; power of UV light = 25 W; reaction time = 50 min.

Effect of Cu(II) concentration

As shown in Figure 1, TC degradation in the PMS/UV and PDS/UV systems with Cu(II) were both higher than that without Cu(II), indicating that the Cu(II) concentration may be one of key factors to influence the oxidative capacity of such systems. As shown in Figure 2, the degradation of TC was 84.0%, 86.9%, 95.4%, 94.7% and 92.8% at 50 min in the Cu(II)/PMS/UV system (top), when the Cu(II) concentration was 5, 15, 30, 50 and 100 μM, respectively. It was found that TC degradation increased with the increased Cu(II) concentration, but TC degradation was decreased slightly when the Cu(II) concentration exceeded 30 μM. Thus, the optimal Cu(II) concentration was 30 μM. Likewise, as shown in Figure 2, the TC degradation followed

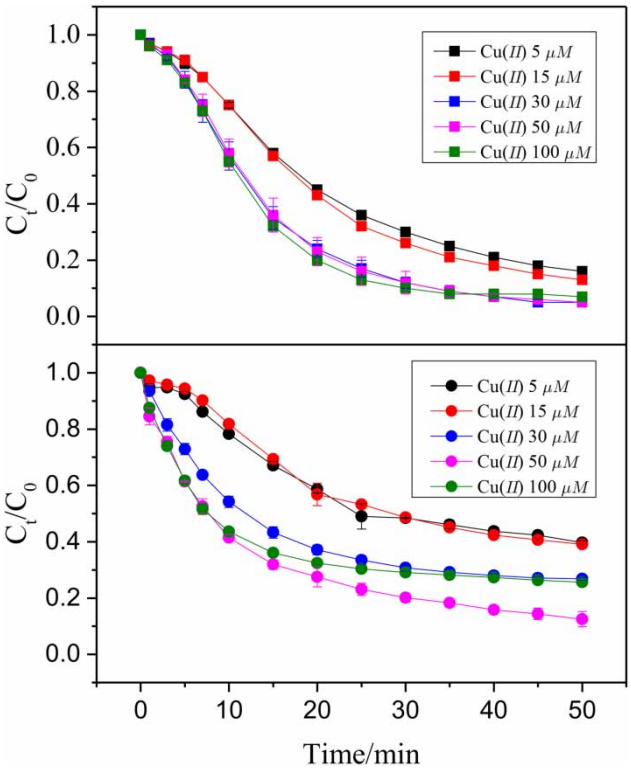

Figure 2 | Effect of Cu(II) concentration in the Cu(II)/PMS/UV (top) and Cu(II)/PDS/UV (bottom) systems. Experimental conditions: $[Cu(II)]_0 = 5$, 15, 30, 50, 100 μM; $[PMS]_0 = [PDS]_0 = 0.50$ mM; $[TC]_0 = 9$ mg/L; pH = 3.5; $T_0 = 25$ °C; power of UV light = 25 W; reaction time = 50 min.

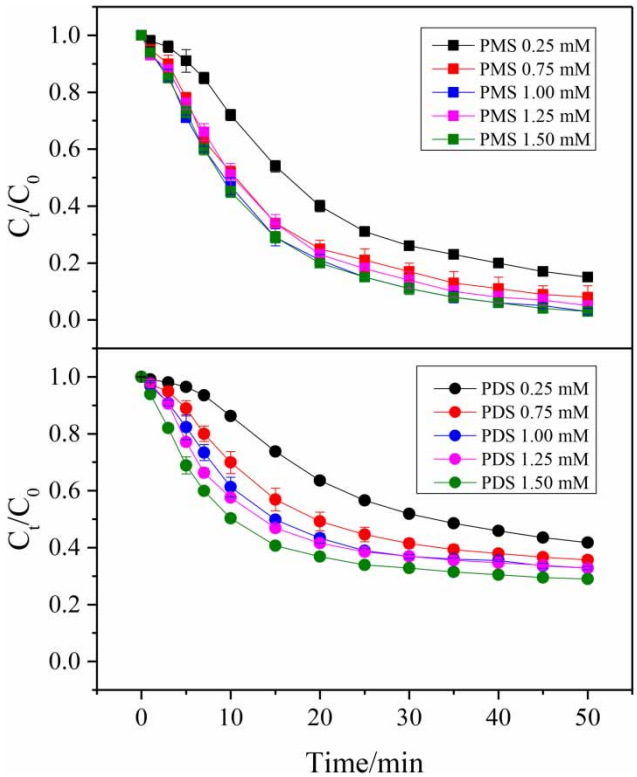

Figure 3 | Effect of oxidative agents concentration in the Cu(II)/PMS/UV (top) and Cu(II)/PDS/UV (bottom) systems. Experimental conditions: $[Cu(II)]_0 = 20$ μM; $[PMS]_0 = [PDS]_0 = 0.25$, 0.75, 1.00, 1.25 and 1.50 mM; $[TC]_0 = 9$ mg/L; pH = 3.5; $T_0 = 25$ °C; power of UV light = 25 W; reaction time = 50 min.

the same rule in the Cu(II)/PDS/UV system (bottom), where the optimal Cu(II) concentration was 50 μM. The enhanced degradation rate with higher Cu(II) concentration for these two systems is likely attributed to the higher amount of Cu(I) and radicals. The phenomenon of much higher Cu(II) concentration may be because excessive Cu(I) reacted with radicals, following Equations (4) and (5) (Buxton *et al.* 1988; Liang & Su 2009).

$$Cu(I) + SO_4^{-}\cdot \rightarrow Cu(II) + SO_4^{2-} \quad (4)$$

$$Cu(I) + \cdot OH \rightarrow Cu(II) + OH^{-} \quad (5)$$

Effect of PMS and PDS concentration

To find the effect of PMS and PDS concentration on TC degradation, different PMS and PDS concentrations were examined in their own systems. As shown in Figure 3, TC removal was 85.0%, 92.1%, 96.6%, 95.2% and 96.8% during 50 min in the Cu(II)/PMS/UV system (top). Clearly, TC degradation was increased with the increasing PMS concentration, which may be because higher PMS concentration could be activated to generate more radicals by UV and Cu(I) at the same time. Based on the above, more free radicals such as $SO_4^{-}\cdot$ and ·OH could remove more TC due to its strong oxidative capacity. Similar to PMS, when the PDS concentration was increased from 0.25 mM to 1.50 mM, TC degradation in the Cu(II)/PDS/UV system (bottom) was increased as well. In general, TC was removed more completely in the Cu(II)/PMS/UV system compared with the Cu(II)/PDS/UV system at the same PMS or PDS concentration.

The reaction mechanism of the Cu(II)/UV system with PMS and PDS

Quenching studies for radical identification

Based on the results above, it is established that the oxidative capacity of the Cu(II)/PMS/UV system is higher than that of Cu(II)/PDS/UV system at the same conditions. One of reasons may be related to the different species of the free radicals that exist in these two systems (Liang & Su 2009; Verma *et al.* 2016). In order to identify the species of

radicals in the Cu(II)/PMS/UV and Cu(II)/PDS/UV systems, experiments involving the addition of TBA and EA were undertaken. TBA, an effective scavenger for •OH, has a higher reaction rate with •OH ($k = 6.0 \times 10^8\ M^{-1}\ s^{-1}$) (Buxton *et al.* 1988) and slightly lower reaction rate with SO_4^{-}• ($k = 8.0 \times 10^5\ M^{-1}\ s^{-1}$) (Neta *et al.* 1988). In contrast, EA is effective for both •OH and SO_4^{-}•, whose reaction rates are 1.2×10^9–$2.8 \times 10^9\ M^{-1}\ s^{-1}$ and 1.6×10^7–$7.7 \times 10^7\ M^{-1}\ s^{-1}$, respectively (Buxton *et al.* 1988; Neta *et al.* 1988). As shown in Figure 4(a), TC degradation was greatly decreased from 93.1% to 28.8% and 23.8% in the Cu(II)/PMS/UV system with TBA and EA (top), respectively, which indicated that •OH was the primary free radical in the Cu(II)/PMS/UV system. TC removal was 54.0% and 27.8% in the Cu(II)/PDS/UV system with TBA and EA compared with 67.1% in the Cu(II)/PDS/UV system. This result showed that a great amount of SO_4^{-}• and a small amount of •OH exist in the Cu(II)/PDS/UV system, following Equation (6) (He *et al.* 2013).

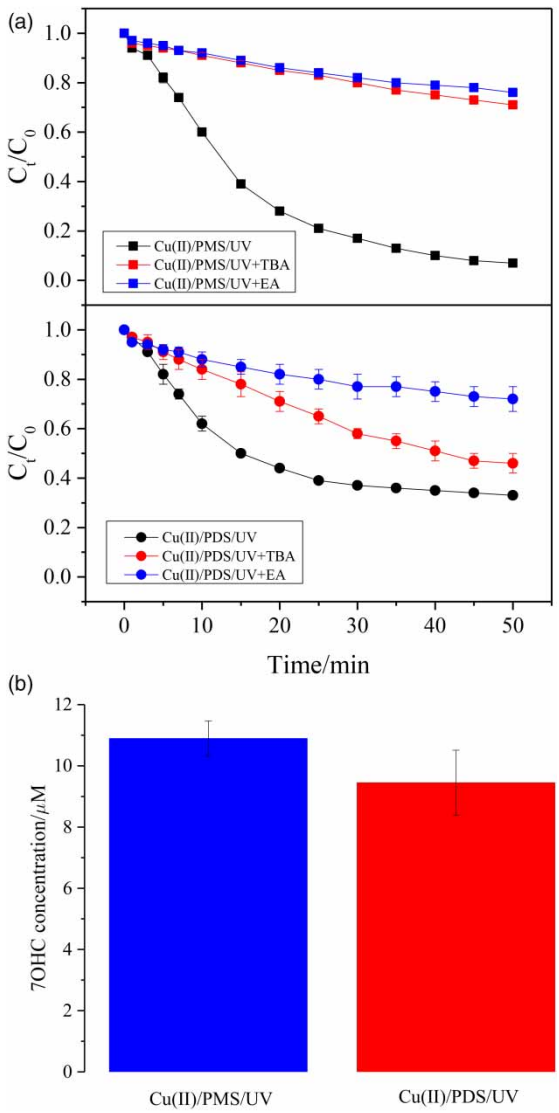

Figure 4 | (a) Effect of the addition of different radical scavengers in the Cu(II)/PMS/UV (top) and Cu(II)/PDS/UV (bottom) systems. (b) The concentration of 7OHC. Experimental conditions: $[Cu(II)]_0 = 20\ \mu M$; $[PMS]_0 = [PDS]_0 = 0.50\ mM$; $[TBA]_0 = 50\ mM$; $[EA]_0 = 50\ mM$; $[coumarin]_0 = 2\ mM$; $[TC]_0 = 9\ mg/L$; pH = 3.5; $T_0 = 25\ °C$; power of UV light = 25 W; reaction time = 50 min.

Besides, from the results of Figure 4(a), •OH may play an important role in these two systems. In order to further determine •OH, coumarin was chosen to capture •OH to generate the fluorescent 7-hydroxycoumarin (7OHC), following Equation (7) (Takuya *et al.* 2011). However, coumarin cannot capture •OH absolutely, so it is a semi-quantitative method to estimate the generation of •OH through the concentration of 7OHC (Zhou *et al.* 2019). As shown in Figure 4(b), the concentration of 7OHC in the Cu(II)/PMS/UV and Cu(II)/PDS/UV systems at 50 min were 10.9 and 9.45 μM, respectively, indicating that •OH was favorable for TC degradation.

$$S_2O_8^{2-} + h\nu \rightarrow SO_4^{-} \cdot + SO_4^{-} \cdot \quad (6)$$

$$\text{Coumarin } C_9H_6O_2 + 2 \cdot OH \rightarrow 7 - \text{hydroxycoumarin } C_9H_6O_3 + H_2O \quad (7)$$

The generation of Cu(I)

It has been proposed that the production of free radicals catalyzed by the copper-redox cycle could strongly enhance the oxidative capacity of the PMS/UV or PDS/UV systems, as shown in Figure 1. Therefore, the generation of Cu(I) may be a key factor to influence the oxidative capacity. The concentrations of Cu(I) in the Cu(II)/PMS/UV, Cu(II)/PDS/UV and Cu(II)/UV systems were detected in order to examine the generation of Cu(I) without the addition of the target compound. As shown in Figure 5, the concentration of Cu(I) in the Cu(II)/PMS/UV and Cu(II)/PDS/UV systems were similar and higher than that in the Cu(II)/UV system, indicating that UV can reduce Cu(II) to Cu(I) at first, and then PMS and PDS can subsequently react with Cu(I) to generate radicals, while Cu(I) is oxidized to Cu(II). Because of this, the copper-redox cycle is formed. According to Equations (1) and (3), the reactions of these two systems can be described by Equations (8)–(10):

$$Cu(II) \xrightarrow{h\nu} Cu(I) \quad (8)$$

$$Cu(I) + HSO_5^{-} \rightarrow Cu(II) + SO_4^{2-} + \cdot OH \quad (9)$$

$$Cu(I) + S_2O_8^{2-} \rightarrow Cu(II) + SO_4^{-} \cdot + SO_4^{2-} \quad (10)$$

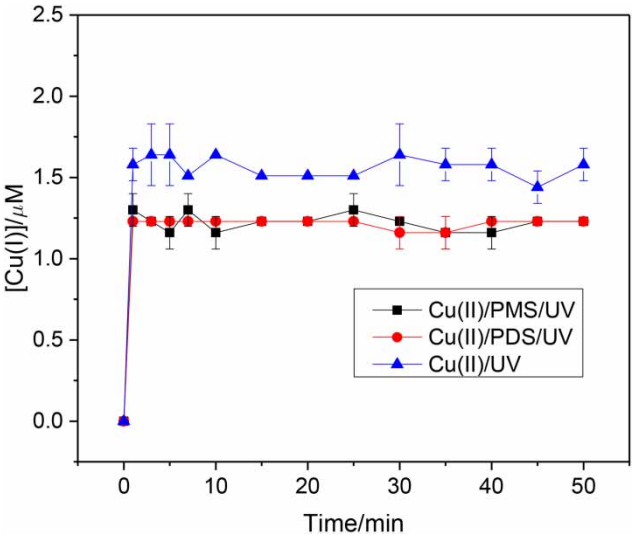

Figure 5 | The concentrations of Cu(I) in the Cu(II)/PMS/UV, Cu(II)/PDS/UV and Cu(II)/UV systems. Experimental conditions: $[Cu(II)]_0 = 20$ μM; $[PMS]_0 = [PDS]_0 = 0.50$ mM; pH = 3.5; $T_0 = 25$ °C; power of UV light = 25 W; reaction time = 50 min.

The role of oxygen

Many studies have shown that oxygen can be activated by UV and transition metals to generate H_2O_2, which is further decomposed to produce •OH (Wen *et al.* 2014; Lee *et al.* 2016). In order to examine the role of oxygen in the Cu(II)/PMS/UV (top) and Cu(II)/PDS/UV (bottom) systems, O_2 or N_2 was continuously bubbled into these two systems. As shown in Figure 6(a), compared with the Cu(II)/PMS/UV (or Cu(II)/PDS/UV) and Cu(II)/PMS/UV/N_2 (or Cu(II)/PDS/UV/N_2) systems, it was observed that the addition of O_2 could enhance the oxidative capacity and increase TC degradation, which was consistent with the former studies. Nevertheless, the degradation of TC was almost the same in the Cu(II)/PMS/UV, Cu(II)/PMS/UV/O_2 and Cu(II)/PMS/UV/N_2 systems, indicating that PMS rather than O_2 is the primary oxidizing agent in the Cu(II)/PMS/UV system. The same results were found in the Cu(II)/PDS/UV system as well. Based on the description above, the reaction mechanism of the Cu(II)/UV system with PMS and PDS can be shown in Figure 6(b).

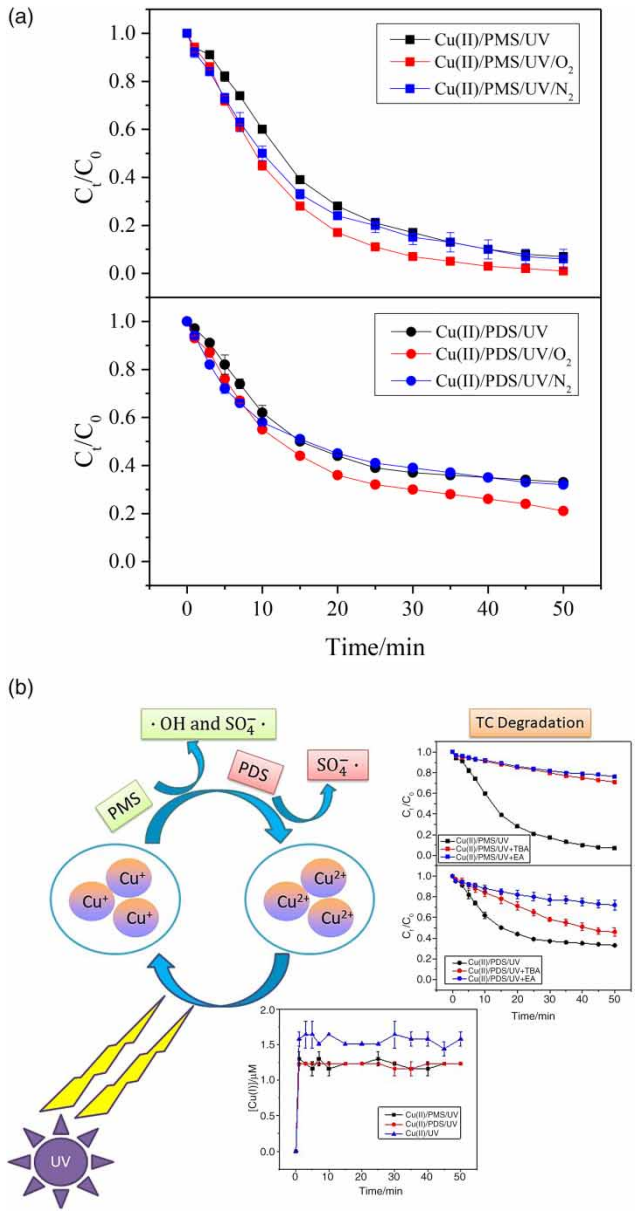

Figure 6 | (a) The role of oxygen in the Cu(II)/PMS/UV (top) and Cu(II)/PDS/UV (bottom) systems. (b) The reaction mechanism of the Cu(II)/UV system with PMS and PDS. Experimental conditions: $[Cu(II)]_0 = 20$ μM; $[PMS]_0 = [PDS]_0 = 0.50$ mM; $[TC]_0 = 9$ mg/L; pH = 3.5; $T_0 = 25$ °C; power of UV light = 25 W; O_2 flow rate = 0.5 L•min^{-1}; N_2 flow rate = 0.5 L•min^{-1}; reaction time = 50 min.

Effect of pH

In order to further investigate the reaction mechanism of the Cu(II)/PMS/UV and Cu(II)/PDS/UV systems, the degradation of TC was examined at different initial pH values ranging from 2.0 to 6.0. As shown in Figure 7, TC degradation was increased with the increasing pH level in the Cu(II)/PMS/UV and Cu(II)/PDS/UV systems, which may be related to the species of the free radicals. According to the results in the section, Quenching studies for radical identification, compared with the Cu(II)/PMS/UV system, TC degradation was higher than that in the Cu(II)/PDS/UV system, indicating that •OH was more effective than SO_4^{-}• in removing TC. Many previous studies showed that SO_4^{-}• could be further converted to •OH at high pH, following Equation (11) (Buxton *et al.* 1988; Guan *et al.* 2011). Thus, more TC was removed at pH 5 and 6 due to the great

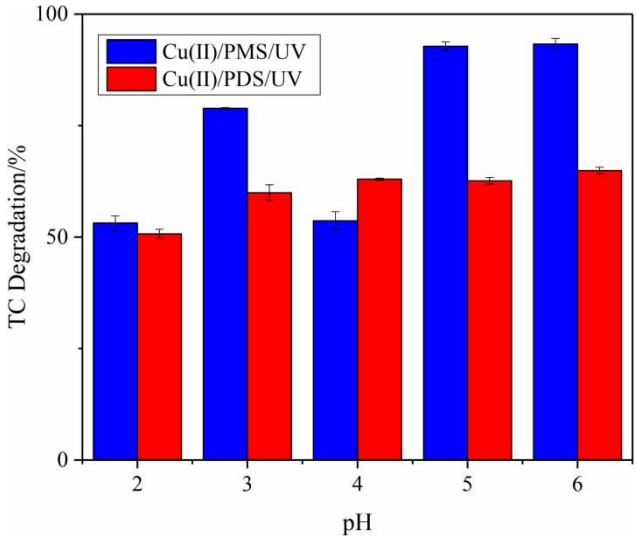

Figure 7 | Effect of different pH in the Cu(II)/PMS/UV and Cu(II)/PDS/UV systems at 50 min. Experimental conditions: $[Cu(II)]_0 = 20\ \mu M$; $[PMS]_0 = [PDS]_0 = 0.50$ mM; $[TC]_0 = 9$ mg/L; pH = 2, 3, 4, 5 and 6; $T_0 = 25\ ^\circ C$; power of UV light = 25 W; reaction time = 50 min.

amount of •OH formed in these two systems. Ji *et al.* (2016) found that deprotonated, non-dissociated TC was more reactive for the generation of $SO_4^{\cdot-}$ because TC has three p*K*a ($pK_{a1} = 3.3$, $pK_{a2} = 7.7$ and $pK_{a3} = 9.7$) and PDS was activated by TC itself. It can be noted that TC degradation at pH 3.0 in the Cu(II)/PMS/UV was higher than that at pH 4.0, which may be likely that pH 3.0 was close to pK_{a1} and the form of TC at pH 3.0 in the system would generate considerable $SO_4^{\cdot-}$.

$$SO_4^{\cdot-} + OH^- \rightarrow SO_4^{2-} + \cdot OH \quad (11)$$

Degradation kinetics

To investigate the degradation kinetics of TC in the Cu(II)/PMS/UV and Cu(II)/PDS/UV systems, different concentrations of TC ranging from 3 to 15 mg/L, were introduced. As shown in Figure 8(a) and 8(b), the TC degradation in these two systems was decreased with the increasing TC concentration, in accordance with the general rule. As shown in Figure 8(a), the degradation of TC during a 50 min period in the Cu(II)/PMS/UV system can be described by the pseudo-first-order kinetics model, and the kinetics equation is grown in Equation (12). The rate constant (k) and correlation coefficient (R^2) in the Cu(II)/PMS/UV system are summarized in Table 1. Moreover, as shown in Figure 8(b), according to reaction time, the TC degradation kinetics in the Cu(II)/PDS/UV system can be divided into two parts: one from 0 to 7 min and

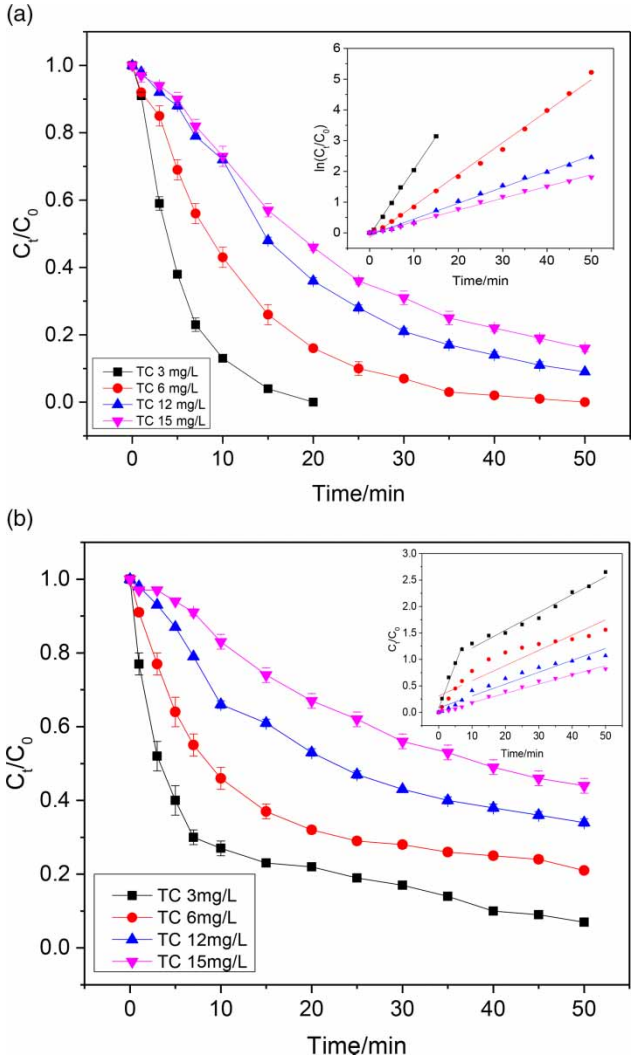

Figure 8 | (a) Effect of TC concentration and linear fit of rate constants from kinetic models for TC degradation in the Cu(II)/PMS/UV system. (b) Effect of TC concentration and linear fit of rate constants from kinetic models for TC degradation in the Cu(II)/PDS/UV system. Experimental conditions: $[Cu(II)]_0 = 20\ \mu M$; $[PMS]_0 = [PDS]_0 = 0.50$ mM; $[TC]_0 = 3$, 6, 12 and 15 mg/L; pH = 3.5; $T_0 = 25\ ^\circ C$; power of UV light = 25 W; reaction time = 50 min.

Table 1 | Pseudo-first-order rate constants for TC degradation in the Cu(II)/PMS/UV system

[TC], mg/L	3	6	12	15
k, min^{-1}	0.206	0.098	0.050	0.038
R^2	0.996	0.993	0.993	0.994

Experimental conditions: $[Cu(II)]_0 = 20\ \mu M$; $[PMS]_0 = 0.50$ mM; $[TC]_0 = 3$, 6, 12 and 15 mg/L; pH = 3.5; $T_0 = 25\ ^\circ C$; power of UV light = 25 W; reaction time = 50 min.

the other from 10 to 50 min. These two parts were in good agreement with the pseudo-first-order kinetics model, respectively. R^2 and k values in the Cu(II)/PDS/UV system are summarized in Table 2, where the rate constants during

Table 2 | Pseudo-first-order rate constants for TC degradation in the Cu(II)/PDS/UV system

	0–7 min				10–50 min			
[TC], mg/L	3	6	12	15	3	6	12	15
k, min^{-1}	0.181	0.086	0.031	0013	0.034	0.017	0.017	0.016
R^2	0.971	0.998	0.975	0.948	0.974	0.934	0.968	0.981

Experimental conditions: $[Cu(II)]_0 = 20\ \mu M$; $[PDS]_0 = 0.50$ mM; $[TC]_0 = 3$, 6, 12 and 15 mg/L; pH = 3.5; $T_0 = 25\ ^\circ C$; power of UV light = 25 W; reaction time = 50 min.

0 to 7 min were higher than that during 10 to 50 min. In addition, compared with the Cu(II)/PDS/UV system, k in the Cu(II)/PMS/UV system was much higher, indicating that TC was removed more quickly in the Cu(II)/PMS/UV system. These results are consistent with the phenomenon in Figures 1 and 4.

$$-\ln(C_t/C_0) = kt \quad (12)$$

CONCLUSIONS

This study investigated TC degradation with Cu(II) and UV in order to compare with the activation of PMS and PDS. The results showed that TC degradation was much higher in the Cu(II)/PMS/UV and Cu(II)/PDS/UV systems via comparison with other different systems. The TC degradation was increased with the increasing Cu(II) concentration, but a much higher Cu(II) concentration may result in more Cu(I) being generated, which could quench the radicals and inhibit TC removal. It was observed that the optimal Cu(II) concentration of the Cu(II)/PMS/UV and Cu(II)/PDS/UV systems were 30 μM and 50 μM, respectively. With the PMS or PDS concentration increasing in their own systems, the TC degradation was increased due to more radicals being generated during the same time period. Quenching studies indicated that •OH was primary free radicals in the Cu(II)/PMS/UV system. However, SO_4^{-}• was the main free radical in the Cu(II)/PDS/UV system where •OH also played an important role. The degradation of TC was increased with increasing pH level. Besides, the degradation of TC in these two systems can be described by the pseudo-first-order kinetics model.

ACKNOWLEDGEMENTS

This work was supported by the National Natural Science Foundation of China (No. 51508353, 51741807, 51878357).

REFERENCES

Ai, C. L., Zhou, D. D., Wang, Q., Shao, X. W. & Lei, Y. J. 2015 Optimization of operating parameters for photocatalytic degradation of tetracycline using In_2S_3 under natural solar radiation. *Solar Energy* **113**, 34–42.

American Public Health Association/American Water Works Association/Water Environment Federation 2005 *Standard Methods for the Examination of Water and Wastewater*, Washington, DC, USA.

Anipsitakis, G. P. & Dionysiou, D. D. 2004 Radical generation by the interaction of transition metals with common oxidants. *Environmental Science & Technology* **38**, 3705–3712.

Bedoui, A., Limem, E., Ahmed, A. & Bensalah, N. 2011 Photo-fenton treatment of actual agro-industrial wastewaters. *Industrial & Engineering Chemistry Research* **50**, 6673–6680.

Buxton, G. V., Greenstock, C. L., Helman, W. P. & Ross, A. B. 1988 Critical review of rate constants for reactions of hydrated electrons, hydrogen atoms and hydroxyl radicals (·OH/·O⁻) in Aqueous Solution. *Journal of Physical and Chemical Reference Data* **17**, 513–886.

Cui, C. Z., Jin, L., Jiang, L., Han, Q., Lin, K. F., Lu, S. G., Zhang, D. & Cao, G. M. 2016 Removal of trace level amounts of twelve sulfonamides from drinking water by UV-activated peroxymonosulfate. *Science of the Total Environment* **572**, 244–251.

Guan, Y. H., Ma, J., Li, X. C., Fang, J. Y. & Chen, L. W. 2011 Influence of pH on the formation of sulfate and hydroxyl radicals in the UV/peroxymonosulfate system. *Environmental Science & Technology* **45**, 9308–9314.

He, X. X., Cruz, A. A. & Dionysiou, D. D. 2013 Destruction of cyanobacterial toxin cylindrospermopsin by hydroxyl radicals and sulfate radicals using UV-254 nm activation of hydrogen peroxide, persulfate and peroxymonosulfate. *Journal of Photochemistry and Photobiology A: Chemistry* **251**, 160–166.

Ji, Y. F., Shi, Y. Y., Dong, W., Wen, X., Jiang, M. D. & Lu, J. H. 2016 Thermo-activated persulfate oxidation system for tetracycline antibiotics degradation in aqueous solution. *Chemical Engineering Journal* **298**, 225–233.

Jorge, R. C., Carlos, A., Tania, S., Dionysios, D. D., Gianluca, L. P., Marco, S. L. & Jose, A. P. 2017 Treatment of winery wastewater by sulphate radicals: HSO_5^{-}/transition metal/UV-A LEDs. *Chemical Engineering Journal* **310**, 473–483.

Kang, D. E., Lim, C. S., Kim, J. Y., Kim, E. S., Chun, H. J. & Cho, B. R. 2014 Two-Photon probe for Cu^{2+} with an internal reference: quantitative estimation of Cu^{2+} in human tissues by two-photon microscopy. *Analytical Chemistry* **86**, 5353–5359.

Khan, S., He, X. X., Khan, H. M., Boccelli, D. & Dionysiou, D. D. 2016 Efficient degradation of lindane in aqueous solution by iron (II) and/or UV activated peroxymonosulfate. *Journal of Photochemistry and Photobiology A: Chemistry* **316**, 37–43.

Kuster, A. & Adler, N. 2014 Pharmaceuticals in the environment: scientific evidence of risks and its regulation. *Philosophical Transactions of the Royal Society B* **369**, 1–8.

Lee, H., Lee, H. J., Seo, J., Kim, H. E., Shin, Y. K., Kim, J. H. & Lee, C. 2016 Activation of oxygen and hydrogen peroxide by copper(II) coupled with hydroxylamine for oxidation of organic contaminants. *Environmental Science & Technology* **50**, 8231–8238.

Liang, C. J. & Su, H. W. 2009 Identification of sulfate and hydroxyl radicals in thermally activated persulfate. *Industrial & Engineering Chemistry Research* **48** (11), 5558–5562.

Liu, W. Q., Fang, C. L., Huang, Y., Ai, L. Y., Yang, F., Wang, Z. H. & Liu, J. S. 2016a Is UV/Ce(IV) process a chloride-resistant AOPs for organic pollutants decontamination? *The Royal Society of Chemistry* **6**, 93558–93563.

Liu, Y. Q., He, X. X., Duan, X. D., Fu, Y. S., Despo, F. & Dionysiou, D. D. 2016b Significant role of UV and carbonate radical on the degradation of oxytetracycline in UV-AOPs: kinetics and mechanism. *Water Research* **95**, 195–204.

Lou, X. Y., Xiao, D. X., Fang, C. L., Wang, Z. H., Liu, J. S., Guo, Y. G. & Lu, S. Y. 2016 Comparison of UV/hydrogen peroxide and UV/peroxydisulfate processes for the degradation of humic acid in the presence of halide ions. *Environmental Science and Pollution Research* **23**, 4778–4785.

Louit, G., Foley, S. & Cabillic, J. 2005 The reaction of coumarin with the OHradical revisited: hydroxylation product analysis determined by fluorescence and chromatography. *Radiation Physics and Chemistry* **72**, 119–124.

Meighan, M., MacNeil, J. & Falconer, R. 2008 Determining the solubility product of $Fe(OH)_3$: an equilibrium study with environmental significance. *Journal of Chemical Education* **85** (2), 254–255.

Natija, B., Hugo, O., Nihal, O., David, H., Abdellatif, G., Salah, A., Enric, B. & Mehmet, A. O. 2017 Kinetics of oxidative degradation/mineralization pathways of the antibiotic tetracycline by the novel heterogeneous electro-Fenton process with solid catalyst chalcopyrite. *Applied Catalysis B: Environmental* **209**, 637–647.

Neta, P., Huie, R. E. & Ross, A. B. 1988 Rate constants for reactions of inorganic radicals in aqueous solution. *Journal of Physical and Chemical Reference Data* **17** (3), 1027–1284.

Oturan, N., Wu, J., Zhang, H., Sharma, V. K. & Oturan, M. A. 2013 Electrocatalytic destruction of the antibiotic tetracycline in aqueous medium by electrochemical advanced oxidation processes: effect of electrode materials. *Applied Catalysis B: Environmental* **140–141**, 92–97.

Shi, W. L., Guo, F. & Yuan, S. L. 2017 *In situ* synthesis of Z-scheme $Ag_3PO_4/CuBi_2O_4$ photocatalysts and enhanced photocatalytic performance for the degradation of tetracycline under visible light irradiation. *Applied Catalysis B: Environmental* **209**, 720–728.

Sun, P. Z., Tyree, C. & Huang, C. H. 2016 Inactivation of *Escherichia coli*, bacteriophage MS2, and *Bacillus* spores under UV/H_2O_2 and UV/peroxydisulfate advanced disinfection conditions. *Environmental Science & Technology* **50**, 4448–4458.

Takuya, M., Masahiro, T. & Makoto, S. 2011 Hydroxyl radical concentration profile in photo-Fenton oxidation process: generation and consumption of hydroxyl radicals during the discoloration of azo-dye Orange II. *Chemosphere* **82**, 1422–1430.

Verma, S., Nakamura, S. & Sillanpaa, M. 2016 Application of UV-C LED activated PMS for the degradation of anatoxin-a. *Chemical Engineering Journal* **284**, 122–129.

Wen, G., Wang, S. J., Ma, J., Huang, T. L., Liu, Z. Q., Zhao, L. & Xu, J. L. 2014 Oxidative degradation of organic pollutants in aqueous solution using zero valent copper under aerobic atmosphere condition. *Journal of Hazardous Materials* **275**, 193–199.

Wu, K. Q., Xie, Y. D., Zhao, J. C. & Hidaka, H. 1999 Photo-Fenton degradation of a dye under visible light irradiation. *Journal of Molecular Catalysis A* **144**, 77–84.

Wu, S. K., Shen, X. P., Zhou, H., Zhu, G. X., Wang, R. Y., Ji, Z. Y., Chen, K. M. & Chen, C. J. 2016 Morphological synthesis of Prussian blue analogue $Zn_3[Fe(CN)_6]_2\ xH_2O$ micro-/nanocrystals and their excellent adsorption performance toward methylene blue. *Journal of Colloid and Interface Science* **464**, 191–197.

Xiao, R. Y., Gao, L. W., Wei, Z. S., Spinney, R., Luo, S., Wang, D. H., Dionysiou, D. D., Tang, C. J. & Yang, W. C. 2017 Mechanistic insight into degradation of endocrine disrupting chemical by hydroxyl radical: an experimental and theoretical approach. *Environmental Pollution* **231**, 1446–1452.

Yang, Y., Pignatello, J. J., Ma, J. & Mitch, W. A. 2014 Comparison of halide impacts on the efficiency of contaminant degradation by sulfate and hydroxyl radical-based advanced oxidation processes (AOPs). *Environmental Science & Technology* **48**, 2344–2351.

Yang, Z. H., Su, R. K., Spinney, R L. S., Cai, M. Q., Xiao, R. X. & Wei, Z. S. 2017 Comparison of the reactivity of ibuprofen with sulfate and hydroxyl radicals: an experimental and theoretical study. *Science of the Total Environment* **590–591**, 751–760.

Ye, T. T., Wei, Z. S., Spinney, R., Tang, C. J., Luo, S., Xiao, R. Y. & Dionysiou, D. D. 2017 Chemical structure-based predictive model for the oxidation of trace organic contaminants by sulfate radical. *Water Research* **116** (1), 106–115.

Yuan, X., Pham, A. N., Xing, G. W., Rose, A. L. & Waite, T. D. 2012 Effects of pH, chloride, and bicarbonate on Cu(I) oxidation kinetics at circumneutral pH. *Environmental Science & Technology* **46**, 1527–1535.

Yuan, X., Pham, A. N., Miller, C. J. & Waite, T. D. 2013 Copper-catalyzed hydroquinone oxidation and associated redox cycling of copper under conditions typical of natural saline waters. *Environmental Science & Technology* **47**, 8355–8364.

Zhang, A. & Li, Y. M. 2014 Removal of phenolic endocrine disrupting compounds from waste activated sludge using UV, H_2O_2, and UV/H_2O_2 oxidation processes: effects of reaction conditions and sludge matrix. *Science of the Total Environment* **493**, 307–323.

Zhang, L., Song, X. Y., Liu, X. Y., Yang, L. Y., Pan, F. & Lv, J. N. 2011 Studies on the removal of tetracycline by multi-walled carbon nanotubes. *Chemical Engineering Journal* **178**, 26–33.

Zhang, R. C., Sun, P. Z., Boyer, T. H., Zhao, L. & Huang, C. H. 2015 Degradation of pharmaceuticals and metabolite in synthetic human urine by UV, UV/H_2O_2, and UV/PDS. *Environmental Science & Technology* **49**, 3056–3066.

Zhou, K. F., Xie, X. D. & Chang, C. T. 2017 Photocatalytic degradation of tetracycline by Ti-MCM-41 prepared at room temperature and biotoxicity of degradation products. *Applied Surface Science* **416**, 248–258.

Zhou, P., Zhang, J. & Zhang, G. C. 2019 Degradation of dimethyl phthalate by activating peroxymonosulfate using nanoscale zero valent tungsten: mechanism and degradation pathway. *Chemical Engineering Journal* **359**, 138–148.

First received 24 July 2018; accepted in revised form 11 January 2019. Available online 23 January 2019